Available online at www.sciencedirect.com
ScienceDirect
Journal of the European Ceramic Society 31 (2011) 1145–1153
www.elsevier.com/locate/jeurceramsoc

Original Article

Effect of intermediate heat treatment on mechanical properties of SiC_f/SiC composites with BN interphase prepared by ICVI

A. Udayakumar [a,*], A. Sri Ganesh [a], S. Raja [b], M. Balasubramanian [c]

[a] *Materials Science Division, National Aerospace Laboratories (Council of Scientific and Industrial Research, India), Bangalore 560 017, India*
[b] *Structural Technologies Division, National Aerospace Laboratories (Council of Scientific and Industrial Research, India), Bangalore 560 017, India*
[c] *Department of Metallurgical & Materials Engineering, Indian Institute of Technology Madras, Chennai 600036, India*

Received 22 March 2010; received in revised form 7 December 2010; accepted 16 December 2010
Available online 13 January 2011

Abstract

SiC_f/SiC composites with BN interface were prepared through isothermal–isobaric chemical vapour infiltration process. Room temperature mechanical properties such as tensile, flexural, inter-laminar shear strength and fracture toughness (K_{IC}) were studied for the composites. The tensile strength of the SiC_f/SiC composites with stabilised BN interface was almost 3.5 times higher than that of SiC_f/SiC composites with un-stabilised BN interphase. The fracture toughness is similarly enhanced to 23 MPa $m^{1/2}$ by stabilisation treatment. Fibre push-through test results showed that the interfacial bond strength between fibre and matrix for the composite with un-stabilised BN interface was too strong (>48 MPa) and it has been modified to a weaker bond (10 MPa) due to intermediate heat treatment. In the case of composite in which BN interface was subjected to thermal treatment soon after the interface coating, the interfacial bond strength between fibre and matrix was relatively stronger (29 MPa) and facilitated limited fibre pull-out.

Keywords: Isothermal–isobaric chemical vapour infiltration; SiC; Boron nitride; Interface; Heat treatment; Tensile properties; SiC_f/SiC composites; Gas turbine engine

1. Introduction

Continuous fibre-reinforced ceramic matrix composites (CF-CMC) such as silicon carbide fibre reinforced silicon carbide ceramic matrix composites (SiC_f/SiC) are prospective candidates for high temperature aerospace applications.[1–6] CF-CMC are being developed for use in high temperature structural applications because of improved flaw tolerance, large work of fracture and non-catastrophic failure, etc.[7,8] They consist of ceramic fibre reinforcement (e.g. fibre tows or cloth layers of carbon, silicon carbide, alumina, etc.) embedded in a ceramic matrix (alumina, carbon, silicon carbide, boron carbide, etc.). The most commonly used CF-CMCs are those comprising of carbon or SiC-based fibre in a carbon or SiC matrix. C_f/C, C_f/SiC and SiC_f/SiC composites are potential candidates for a variety of applications in the aerospace field, including rocket nozzles, gas turbine engines, heat shields and aircraft braking systems, etc.

CF-CMC show a non-linear stress–strain behaviour attributable to various damage/structural fracture phenomena that occur on a microscopic scale, when fibre/matrix bonding is properly tailored during the processing.[2,9] Interfacial bond strength is controlled through the use of a thin film of a compliant material having low shear strength, which is applied on the fibre surface prior to matrix infiltration. Pyrolytic carbon (P_yC) and boron nitride (BN) are the two widely reported interface materials.[10–13] An alternative concept of multilayered interfaces such as $(PyC–SiC)_n$ or $(BN–SiC)_n$ have been developed to improve the mechanical properties, stability and oxidation resistance of SiC_f/SiC composites.[14–17] The key function of an interface material is to arrest and/or deflect the matrix micro cracks that develops under load around the fibre,[10,6,18] to assist the load transfer, and serve as a diffusion barrier layer.[19] BN interface has several advantages over carbon interface as its oxidation starts at a reasonably higher temperature (800 °C) compared to carbon (400 °C). The formation of vitreous B_2O_3

* Corresponding author. Tel.: +91 08 25086750; fax: +91 08 25270098.
E-mail address: audayk@yahoo.com (A. Udayakumar).

0955-2219/$ – see front matter © 2010 Elsevier Ltd. All rights reserved.
doi:10.1016/j.jeurceramsoc.2010.12.018

by the oxidation of BN interface at high temperatures leads to self-healing properties.[20,21]

It is known from literature that BN interface obtained from BCl_3–NH_3 gas mixtures is often poorly crystallised when deposited at low temperatures and pressures (standard CVI conditions) and consequently it reacts with oxygen and moisture.[22–27] Despite this drawback, BN interface has been used in SiC_f/SiC composites[28–34] for many years, since it has superior oxidation resistance than P_yC interface at comparable temperatures of use (500–600 °C). The poor oxidation resistance of BN above 600 °C and its moisture sensitivity are attributed to the poorly crystallised nature of the deposited turbostratic BN interface layers.

Some studies have been therefore carried out on post-deposition heat treatments at high temperatures ranging from 1000 to 1700 °C[26,35] to reduce the reactivity of the boron nitride with oxygen. The stability is obtained by decomposing un-reacted species in the deposited BN interface and by increasing the degree of crystallisation of BN. In the present study, BN interface has been considered and SiC_f/SiC composites have been prepared through CVI process with BN interface. Post-deposition treatment had been done at 1200 °C soon after the BN interface coating in one case and after 430 h of SiC matrix infiltration in the other case. 1200 °C was selected as post deposition temperature, since the fibres start to degrade at higher temperatures.[36–38] The effect of an intermediate heat treatment on the mechanical properties of composites have been studied.

2. Experimental procedure

Three types of SiC_f/SiC composites were prepared through ICVI process using ceramic grade Nicalon 8-Harness satin fabric layers with [0°/90°] fibre orientation. First composite has CVI-derived BN interface (composite A), second composite has CVI-derived BN interface and the composite was subjected to intermediate heat treatment at 1200 °C in argon (Ar) atmosphere for 5 h after 430 h of SiC matrix infiltration (composite B), and the third composite with BN interface stabilised at 1200 °C in Ar atmosphere for 5 h prior to SiC matrix infiltration (composite C). In all the cases, the fibre preform were taken out of the reactor after the BN coating, for exposing it to atmospheric air for 2 h to enhance the crystallinity of deposited BN at relatively low temperature during stabilisation treatment.[24] Layered fibre preform of dimension 250 mm × 220 mm × 5 mm was used for the present study. The gaseous precursors used were 99% pure boron tri-chloride (BCl_3, Praxair, Belgium) and 99% pure ammonia (NH_3, Praxair, Belgium) for BN deposition and 99.8% pure methyl tri-chlorosilane (MTS-CH_3SiCl_3 – Spectrochem, Mumbai, India) and 99.999% pure hydrogen (Inox Air Products, USA) for SiC infiltration. The BN interface was deposited for 3 h on the fibre surface by the CVD reaction between BCl_3 and NH_3 with mass flow rate ratio of 1:1 at l–2 mbar at 850 °C. SiC matrix was obtained by thermally cracking MTS vapour in the presence of hydrogen as carrier/catalyst gas with mass flow rate ratio of 1:16 (e.g. 1.24 l/min MTS and 20 l/min H_2) at 1–2 mbar pressure, between 950 and 980 °C. The composite laminates were densified up to 90% of theoretical density (TD) with frequent interruption of densification cycles for surface machining to enhance the infiltration rate. The schematic representation of ICVI setup used for this study is shown in Fig. 1.

The density and porosity of SiC_f/SiC composites were determined by Archimede's method as per EN1389: 2003 standard procedure. The thin sections (cross-section) derived from all the three types of composites were polished down up to 1 μm finish using diamond suspensions and analysed the microstructure using field emission scanning electron microscopy – FESEM (Carl Zeiss, Supra 40 VP).

To evaluate the interfacial shear strength between the fibre and the matrix of the composites, single fibre push through test was performed using a nanoindenter with nano-positioning system (Nanoindenter G200-MTS Nano Instruments) which has a diamond indenter. Composite sample (cross section) of thickness 1.5 mm was mounted on the epoxy which has a blind hole of diameter ∼5 mm at the center to enable the fibres to be pushed out. Then the samples are reduced to a final thickness of ∼350 μm by mechanical polishing with mirror finish using diamond slurry. The schematic representation of the specimen preparation for single fibre push-through test is shown in Fig. 2. With the nano-positioning system with appropriate optics, individual fibres are selected and load was applied at a rate of 10 μN/s, where the fibres bear the load at the beginning and then slips through the matrix once the force balance between the frictional force and applied force is achieved and then pushed out of the matrix. As the fibre starts slipping, the indenter tip touches the matrix and takes the maximum load which is followed by the unloading cycle. The sequence of fibre push through test is shown in Fig. 3. The force (F) at which the fibre starts slipping is used to calculate the interfacial shear strength (τ_i) from the following Eq. (1).

$$\tau_i = \frac{F}{2\pi r t} \quad (1)$$

where τ_i is the interfacial shear strength (MPa), F is the force at which the fibre starts to slip through the matrix (N), r is the radius of the reinforced fibre (m), and t is the thickness of the sample (m).

The dog-bone tensile test specimens (from all the three types of composites) measuring 102 mm (length) and 22 mm (width) were prepared using water jet cutting machine (HWM-6025-1/2D, Waricut cutting systems, Germany) with a finished gauge section measuring 25 mm long, 6 mm wide and 4.5 mm thick. After machining, the SiC_f/SiC composites were seal coated with SiC by ICVI method. All the cut surfaces were polished and the edges of the test specimens were chamfered. Tensile strength was determined at room temperature using the universal testing machine (5500J 7966, Instron, UK) at a strain rate of 0.1 mm/min.

Flexural test specimens measuring 60 mm in length, 6 mm in breadth, and 4.5 mm in thickness were prepared from composite A and composite B through water jet cutting. The cut surfaces and edges of the samples were polished to get smooth edges. Room temperature flexural strength was determined by 3-point

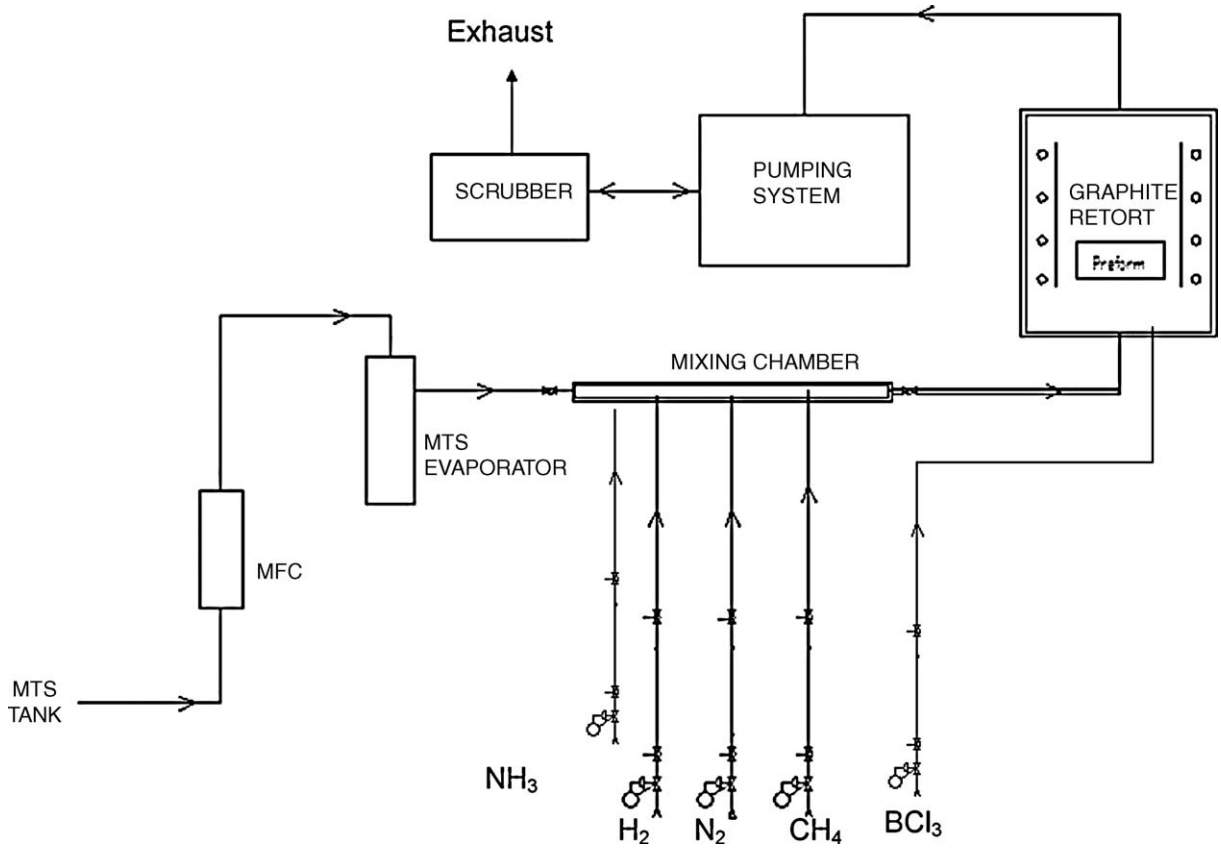

Fig. 1. Schematic diagram of the ICVI setup used for fabrication of SiC_f/SiC composites.

bending with span length of 40 mm using the universal testing machine (Bi-01-138, Bangalore Integrated Systems Solutions, Bangalore) according to ASTM C1341 standard.

All faces of bar specimens (60 mm length × 6 mm width × 4.5 mm thick) were polished down to 1 μm using diamond slurry. A crack was created through thickness by cutting with 0.3 mm thick diamond wheel and then sharpened by number of passes with a razor blade in conjunction with 0.25 μm diamond suspension. The crack depth was measured using a traveling microscope. These single-edge-notched beam (SENB)

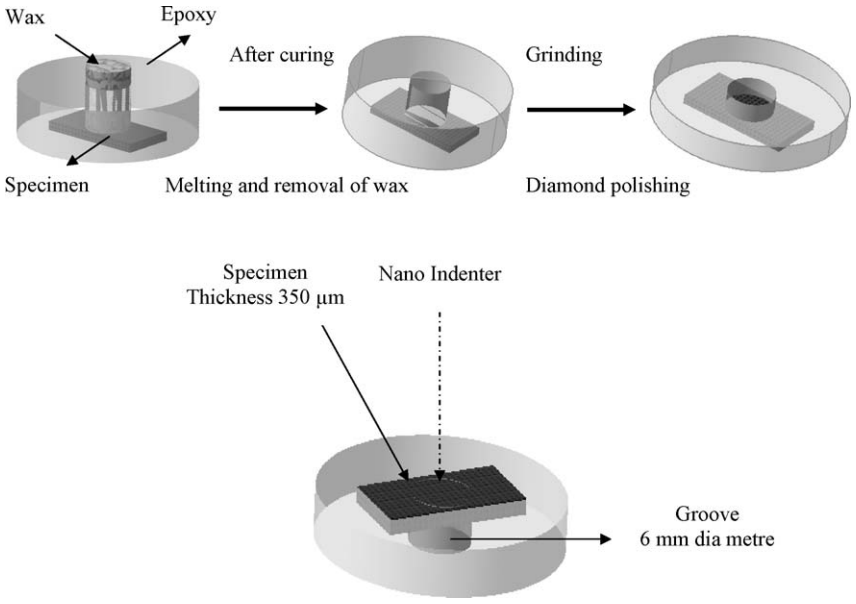

Fig. 2. Schematic flow of specimen preparation for single fibre push-through test.

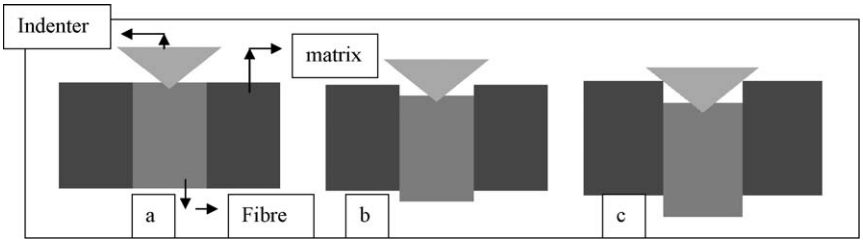

Fig. 3. Schematic representation of sequence of fibre push through test using nano indentation: (a) fibre bearing the load, (b) fibre slipping through and (c) matrix taking load.

specimens were loaded in 3-point bending configuration using the universal testing machine (Bi-01-138, Bangalore Integrated Systems Solutions) and their breaking loads were measured. The K_{IC} values were determined using Eq. (2).[39]

$$K_{IC} = \left(\frac{3Pl}{2bw^{3/2}}\right)\left[1.93 - 3.07\left(\frac{a}{w}\right) + 1.45\left(\frac{a}{w}\right)^2 - 25.07\left(\frac{a}{w}\right)^3 + 25.8\left(\frac{a}{w}\right)^4\right] \quad (2)$$

where P, load; l, support span; b, thickness of the sample; w, width of the sample and a, crack depth.

Short bar specimens measuring 30 mm in length, 8 mm in width and 4 mm in thickness were prepared and inter-laminar shear strength (ILSS) was determined as per ASTM (D 2344/D 2344M) standard. Fracture surfaces of tensile strength tested samples were also analysed using scanning electron microscope (440i, Leo, U.K.) and field emission scanning electron microscopy – FESEM (Carl Zeiss, Supra 40 VP) to get the evidence of fracture processes. In addition, carefully generated fracture surfaces of all the composites were studied by FESEM to analyse the interface.

3. Results and discussion

The density of all types of composites was found to be in the range 2.6–2.7 g/cc.

The SEM micrographs of the cross section of all the composites (composite A, composite B, and composite C) are shown in Fig. 4. In the case of composite A, the interface is not clearly visible and it is very thin (~100 nm). The interface might have reacted with moisture and subsequently with the matrix causing the strongest bond (>48 MPa) between the fibre and the matrix. This is also reflected in the fracture surface micrograph shown in Fig. 5a. Also, it is very clear from Fig. 5a that the interface has reacted and not facilitated the fibre pull out. In the case of composite B, interface is clearly seen and it is significantly thicker (~400 nm) compared to composite A. It is also observed that the interface coating is relatively uniform and the fibre edges have undergone some brittle failure. The interface is constrained to a large extent after 430 h of SiC matrix infiltration and it resulted in a porous interface and modified the strongest bond between the fibre and the matrix to a weak bond to facilitate the fibre de-bonding. The fracture surface micrograph obtained for composite B as shown in Fig. 5b clearly shows the extensive fibre pull out and the pulled out fibre surface looks relatively smooth supporting the moderate interfacial bond strength (10 MPa) between the fibre and matrix. The interface region is seen clearly in composite C and its thickness (~230 nm) is found to be higher than the interface thickness in composite A and lesser than the interface thickness in composite B. The fracture surface micrograph

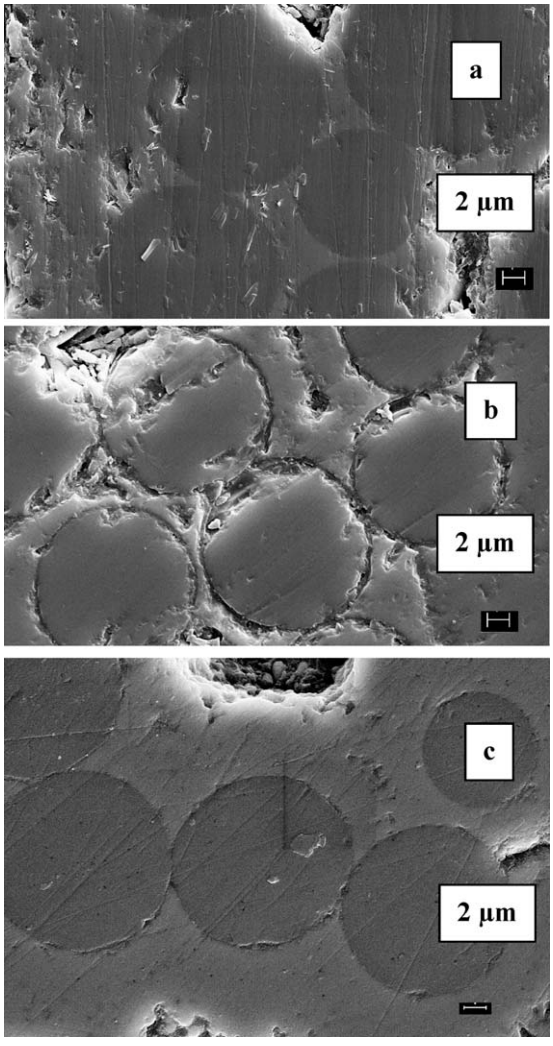

Fig. 4. FESEM micrographs obtained for SiC_f/SiC composites: (a) composite A, (b) composite B, and (c) composite C.

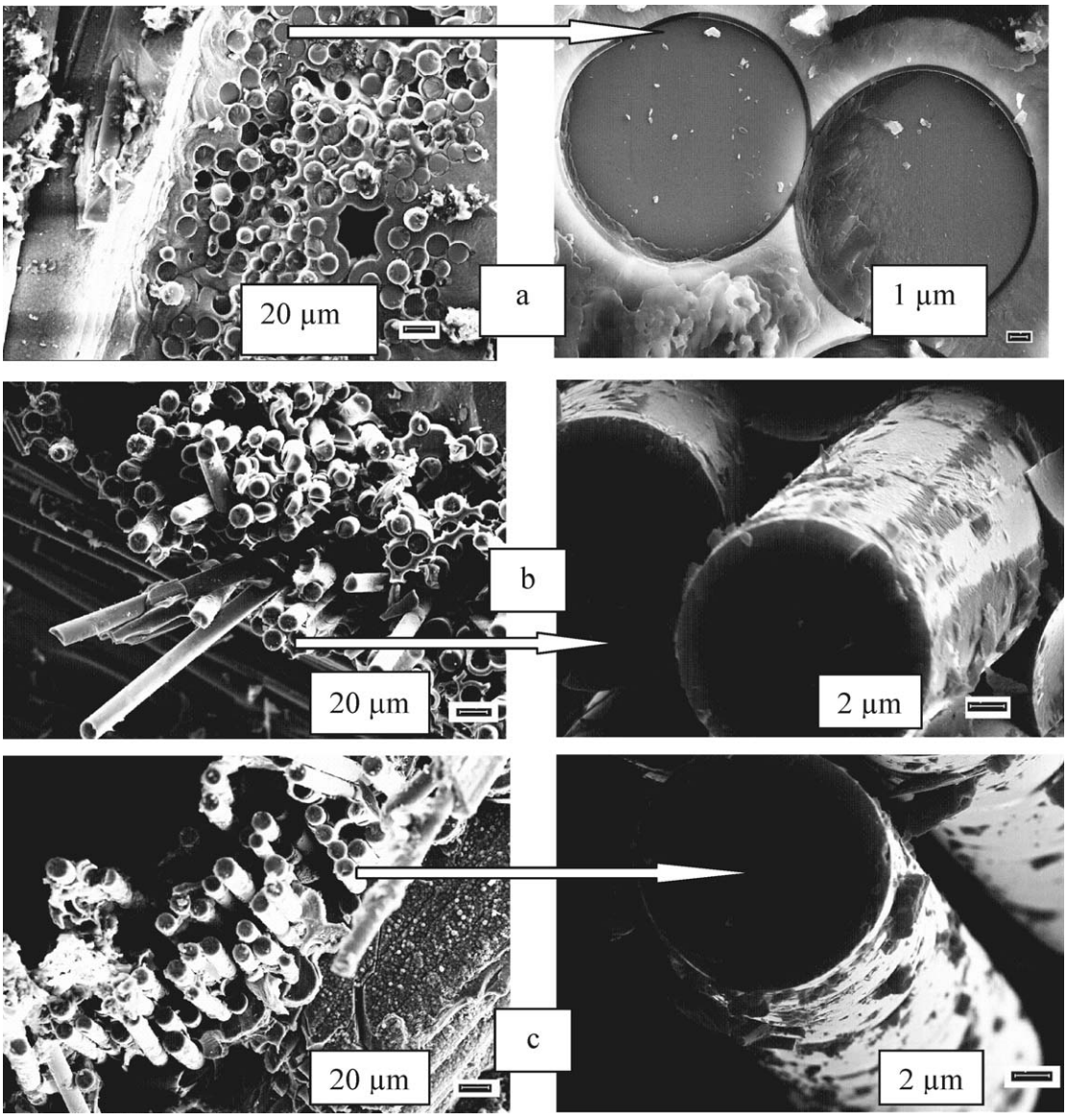

Fig. 5. Scanning electron micrographs of fracture surfaces of SiC_f/SiC composites: (a) composite A, (b) composite B and (c) composite C.

obtained for composite C as shown in Fig. 5c clearly shows the limited fibre pull out and the pulled out fibre surface looks rough supporting the strong interfacial bond strength between the fibre and matrix. A carbon interlayer between the fibre and interface is also expected to be present in all the three types of composites due to thermal decomposition (during heating of the preform) of sizing agent (poly-vinyl alcohol) present on the fibre surface.

From the stress–displacement trend obtained from tensile tests carried out on all the types of composites as seen in Fig. 6, the intermediate heat treatment given to composite B has modified the interfacial bonding between the fibre and matrix. Subsequently, the tensile strength was increased from 70 MPa (composite A) to 233 MPa and thereby changed the brittle composite into a tough composite. Composite A showed very low tensile strength and failed in catastrophic and brittle manner due to the strongest bond between fibre–matrix and very thin interface. It has been reported that the BN deposited at low temperature and low pressure changes to ammonium borate hydrates as a result of reaction with moisture.[25] This could have happened in the present case during loading/unloading of composites into/from reactor when CVI cycles are interrupted for surface machining, to open-up the pore closures in order to enhance the infiltration. The higher strength observed in the case of composite B is also due to the higher interface thickness as already reported elsewhere.[40–42] It was observed that the composite C has exhibited higher tensile strength of 200 MPa with non-linear failure behaviour. The matrix cracking stress was also higher for composite C (∼120 MPa). The percentage elongation obtained for composite A, composite B and composite C were 0.14%, 4.5% and 1.1% respectively.

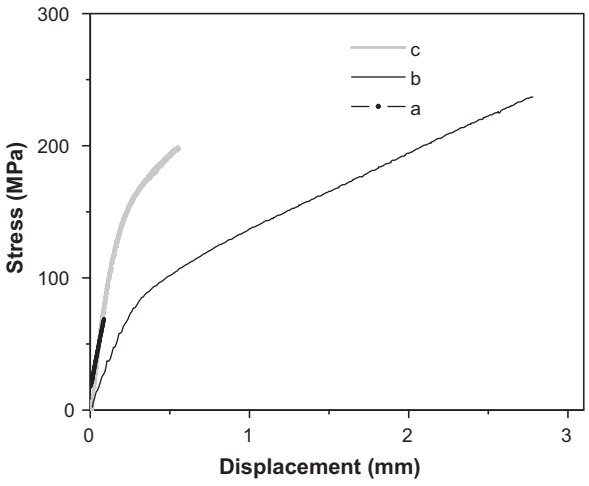

Fig. 6. Typical stress versus displacement curve obtained during tensile testing of SiC_f/SiC composites: (a) composite A, (b) composite B and (c) composite C.

From the SEM micrograph shown in Fig. 7a, composite A showed practically no fibre pull out thereby supporting the low toughness obtained for these composites. It can be due to the formation of strong interface bonding between the fibre-interface and interface-matrix because of the reaction with moisture. It is very clear from the tensile test and fracture surface micrograph results shown in Fig. 6b and 7b that the intermediate heat treatment has improved the crystallinity and stability of BN in the composite B to some extent and modified the bonding strength between the interface and the matrix to a bond weak enough to facilitate good fibre pullout. Medium fibre pull out was seen for the composite C (Fig. 7c) and it is also supporting the lower percentage elongation obtained for these composites. It was observed that out of all these composites, composite B has given better tensile properties. Hence, the composite B was further studied for properties such as interfacial shear strength, flexural strength, fracture toughness and ILSS and compared with composite A.

The indentation curves obtained from single fibre push through tests carried out on composite A, composite B and composite C are shown in Fig. 8. At first, indenter made inroads into fibre during process X (Fig. 8a–c). The gradient changes labeled "push through" in Fig. 8b and c indicates the initiation of interfacial debonding. This result is similar to the result reported by Marshall and Evans.[7] Crack between fibre and matrix propagated and the fibre was elastically deformed and pushed through during the process Y. As the fibre slips through the matrix, indenter is subsequently touching the matrix and the matrix bears the load. Finally, the unloading process Z is seen. The interfacial shear strength (τ_i) was calculated (10 MPa) for the composite B, is weak enough to facilitate the fracture processes in the composites. The fibres subjected to push through test and the signatures of fibre slipping (*f*) were also seen in the respective optical micrograph (Fig. 8b). In the case of composite A, the fibre slipping was not observed indicating a strong bonding between the fibre and matrix (>48 MPa – calculated by taking the maximum load in the indentation curve). The unloading process Z was obtained without fibre slipping (process Y) because

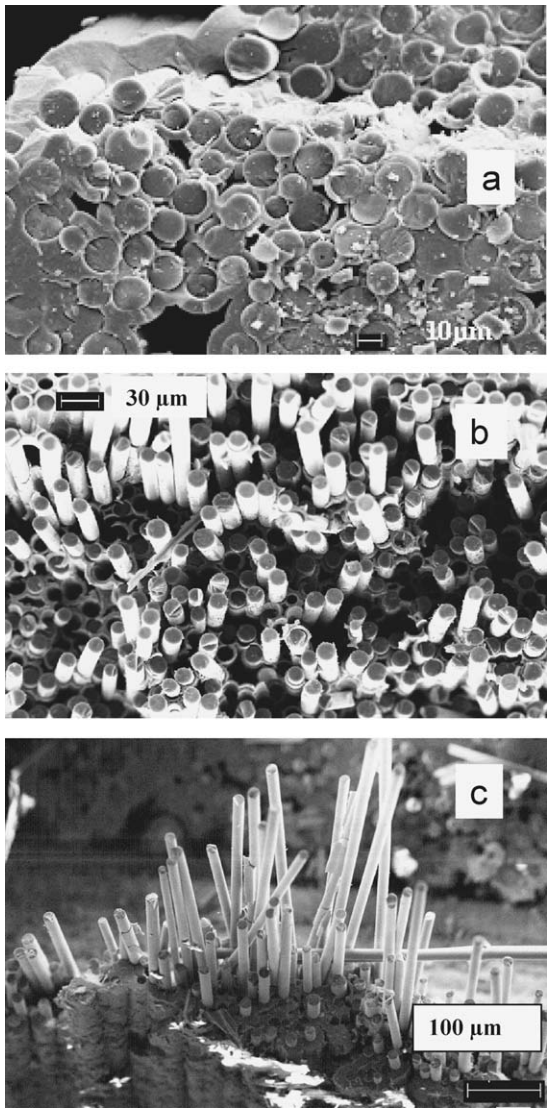

Fig. 7. Scanning electron micrographs of tensile fracture surfaces of SiC_f/SiC composites: (a) composite A showing minimal fibre pull out, (b) composite B showing extensive fibre pull out and (c) composite C showing medium fibre pull out.

of the limitation in maximum load capacity of the nanoindenter. The fibres (*f*) subjected to push through test were shown in Fig. 8a. The signatures of fibre slipping were not observed in the respective optical micrograph (Fig. 8a). It is now confirmed that the intermediate heat treatment has modified the bond strength. The interfacial shear strength (τ_i) obtained for the composite C was 29 MPa indicating the strong bond between fibre and matrix. It also supports the tensile results and fracture micrographs obtained for composite C (Figs. 5c, 6c and 7c). The fibres subjected to push through test and the signatures of fibre slipping (*f*) were also seen in the respective optical micrograph (Fig. 8c).

From the flexural test results obtained on composites A and B (Fig. 9), the mechanical behaviour is linear elastic till the fracture and the failure is sudden in the case of composite A. On the other hand, the composite B exhibited a different mechanical behaviour, which is initially linear elastic followed by a

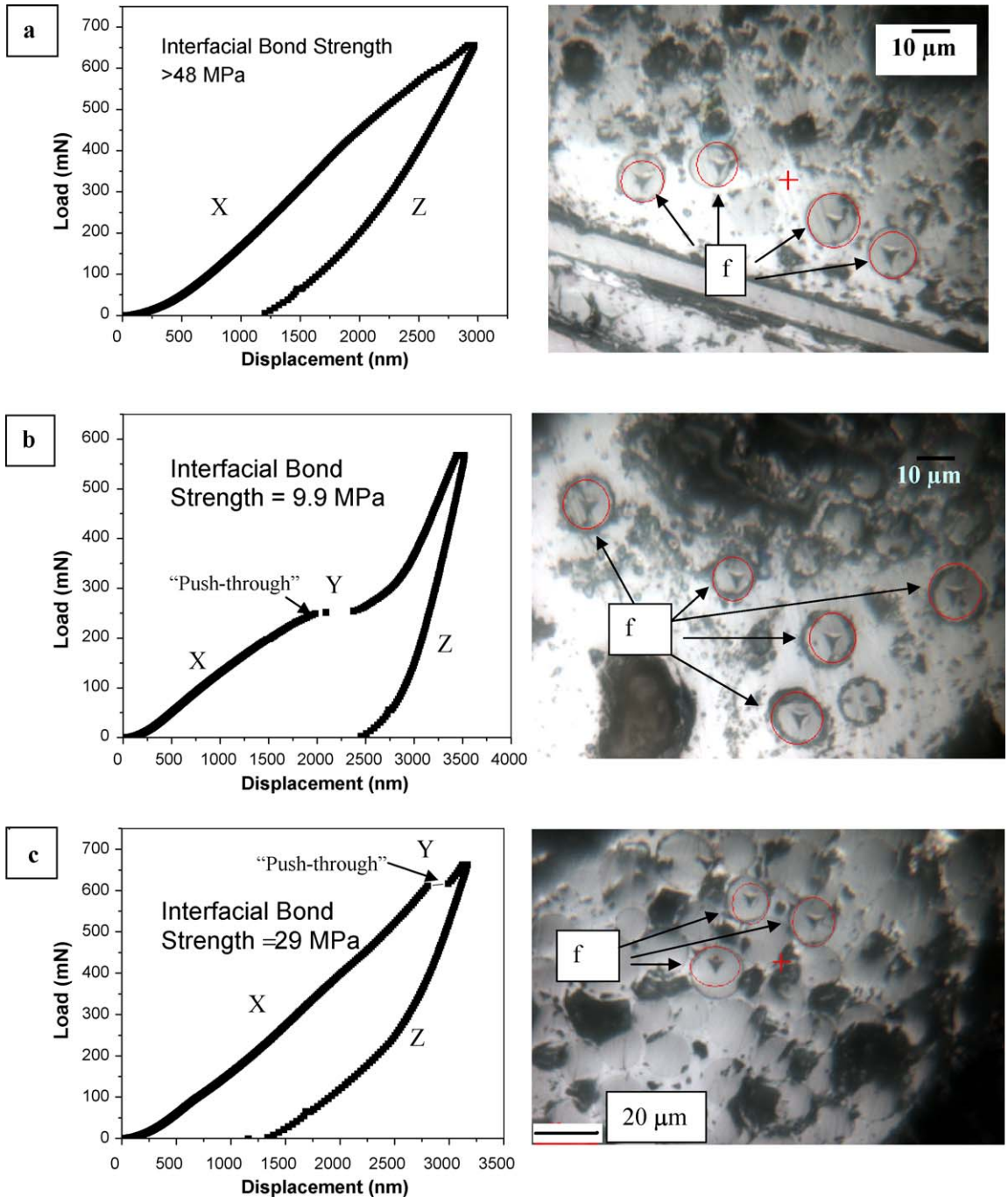

Fig. 8. Indentation load versus displacement plot and optical micrograph obtained for SiC_f/SiC composites after fibre push through test: (a) composite A, (b) composite B, and (c) composite C.

non-linear region reflecting matrix damage (Fig. 9). After reaching the maximum load, the composite B is found to fail layer by layer. From the above results we can conclude that the heat treatment has improved the flexural strength of the composites quite remarkably.

The fracture toughness calculated from Eq. (2) for the composite B is 23 MPa $m^{1/2}$ which is about two times that of composite A, and almost five times than that of typical monolithic SiC. The fracture toughness differences between composite A and composite B could be attributed to the fracture processes which are operating in composite B because of the tailored interface. This is achieved mainly due to the intermediate heat treatment which has stabilised the BN interface. The load versus displacement curves obtained during K_{IC} test (Fig. 10) is clearly demonstrating the higher fracture toughness of composite B. The ILSS of composite B is 21 MPa which is slightly higher than that of composite A (19 MPa) (Fig. 11). The ILSS needs to be improved and the layer by layer failure has to be understood to tailor the composites for better ILSS properties. All the properties obtained for both composites A and B are

Table 1
Typical properties of SiC_f/SiC composites.

Sl. no.	Properties	Composite A	Composite B
1.	Density (g/cc)	2.6–2.7	2.6–2.7
2.	Porosity (%)	10–12	10–12
3.	Reinforcement	Nicalon CG BD woven cloth, 8H satin	Nicalon CG BD woven cloth, 8H satin
4.	Fibre volume V_f (%)	40	40
5.	Matrix Phase	β-Phase with no co-deposition of C or Si	β-Phase with no co-deposition of C or Si
6.	Tensile strength (MPa)	70	233
7.	Flexural strength (MPa)	142	285
8.	Fracture toughness – K_{1C} (MPa $m^{1/2}$)	12	23
9.	Interlaminar shear strength (MPa)	19	21
10.	Percentage elongation	0.14%	4.5%

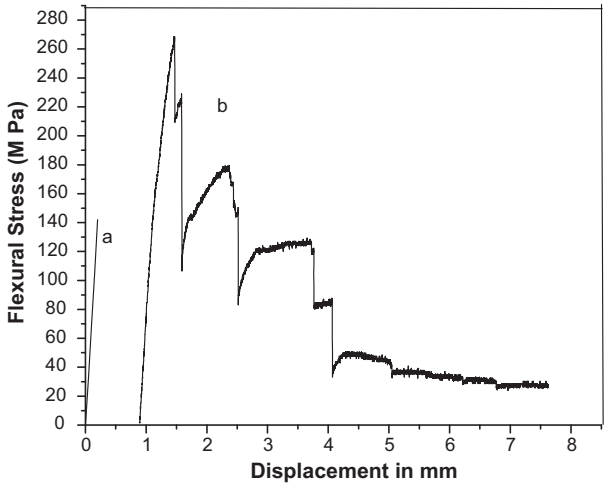

Fig. 9. Flexural test (3 point bend test) results obtained for SiC_f/SiC composites: (a) composite A and (b) composite B.

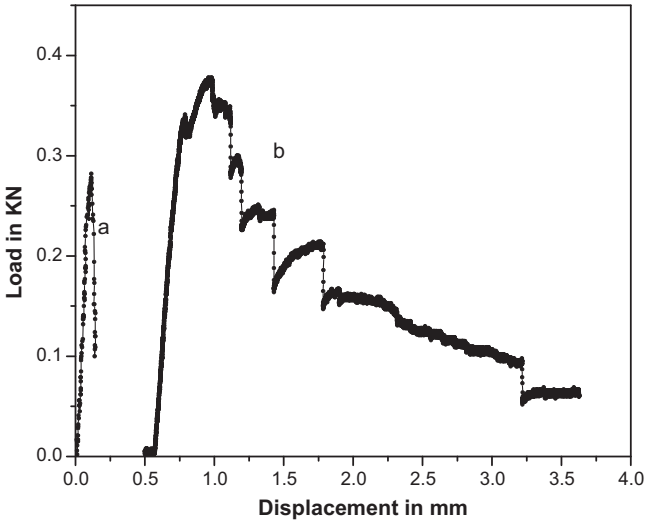

Fig. 10. Load versus displacement curves obtained during K_{IC} test (3 point bending of SENB composite specimens) for SiC_f/SiC composites: (a) composite A and (b) composite B.

listed in Table 1. It is evident from Table 1 that the intermediate heat treatment step introduced in the case of composite B has fairly improved the mechanical properties.

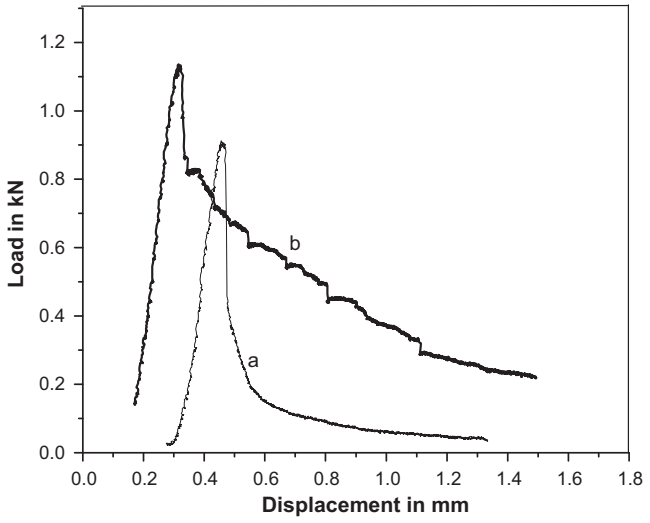

Fig. 11. Load versus displacement curves obtained during ILSS test for SiC_f/SiC composites: (a) composite A and (b) composite B.

4. Conclusion

Intermediate heat treatment of SiC_f/SiC laminates at 1200 °C for 5 h in argon atmosphere improves the mechanical properties of the composites. A threefold increase in tensile strength (233 MPa) and two fold increase in fracture toughness (23 MPa $m^{1/2}$) is achieved by the intermediate heat treatment given after 430 h of SiC matrix infiltration. The superior properties obtained for the SiC_f/SiC composites subjected to intermediate heat treatment are directly attributable to the improvement in the interface quality. It is concluded that the interfacial bond strength between fibre and matrix had been modified to that of a weak bond (10 MPa) by the intermediate heat treatment and facilitated the fibre debonding and other fracture processes such as crack bridging and fibre pull out in the composites leading to better mechanical properties. SiC_f/SiC composites with the BN interface subjected to stabilisation heat treatment at 1200 °C for 5 h in argon atmosphere prior to matrix infiltration showed intermediate tensile strength (200 MPa) and lower percentage of elongation (1.1%).

Acknowledgements

The authors thank Mr. M.A. Venkataswamy and his group for the SEM studies, Mr. P. Kumara, Ms. L. Priya, Mr. S. Ganesh, Mr. M. Suresh and Ms. M.V. Geetha for their help in carrying out the experiments, Mr. S. Kalyana sundaram for mechanical testing and Dr. K.S. Raja, Dr. Harish Barshilia and group for FESEM and Raman Spectroscopic analysis. Thanks are due to Dr. Rajendra Alevoor and Mr. Hari Krishna for their support in carrying out single fibre push-through test. The authors record sincere thanks to Mr. M.K. Sridhar for his continuous support and encouragement. Thanks are due to Dr. Nick.J. Archer and Mr. John Yeatman from M/s. Archer Technicoat Limited, UK for their support and suggestions. The authors also thank the Director, NAL for his active support and constant encouragement. Financial support from DMRL is gratefully acknowledged.

References

1. Bansal NP. *Handbook of ceramic composites*. Kluwer Academic Publisher; 2005.
2. Chawla KK. *Ceramic matrix composites*. London: Chapman and Hall; 1993.
3. Tressler RE. Recent developments in fibres and interphases for high temperature ceramic matrix composites. *Compos Part A: Appl Sci Manuf* 1999;**30**:429.
4. Morscher GN. Tensile stress rupture of SiC_f/SiC_m mini composites with carbon and boron nitride interphases at elevated temperatures in air. *J Am Ceram Soc* 1997;**80**:2029.
5. Naslain R, Langlais F. Chemical vapor deposition processing of ceramic–ceramic composite materials. *Mater Sci Res* 1986;**20**:145.
6. Faber KT. Ceramic composite interfaces: properties and design. *Annu Rev Mater Sci* 1997;**27**:499.
7. Marshall DB, Evans AG. Failure mechanisms in ceramic–fibre/ceramic matrix composites. *J Am Ceram Soc* 1985;**68**:225–31.
8. Evans AG, Marshall DB. The mechanical behaviour of ceramic matrix composites overview no. 85. *Acta Metall* 1989;**37**:2567–83.
9. Aveston J, Cooper GA, Kelly A, Proceedings Properties of Fibre Ltd., 1971. *Composites, national physics laboratory*. IPC Science and Technology Press; 1971. p. 15–26.
10. Kerans RJ, Hay RS, Parthasarathy TA, Cinibulk MK. Interface design for oxidation resistant ceramic composites. *J Am Ceram Soc* 2002;**85**: 2599.
11. Singh RN, Brun MK. Effect of boron nitride coating on fibre–matrix interactions. *Ceram Sci Eng Proc* 1987;**8**:634.
12. Naslain RN, Dugne O, Guette A, Sevely J, Brosse CR, Rocher JP, Cotteret J. Boron nitride interface in ceramic matrix composites. *J Am Ceram Soc* 1991;**74**:2482.
13. Patibandla N, Luthra K. Chemical vapor deposition of boron nitride. *J Electrochem Soc* 1992;**139**:3558.
14. Droillard C, Lamon J. Fracture toughness of 2-D woven SiC_f/SiC CVI composites with multilayered interphases. *J Am Ceram Soc* 1996;**79**:849–58.
15. Droillard C, Lamon J, Bourrat X. Strong interface in CMCs, a condition for efficient multilayered inter-phases. *Mater Res Soc Proc* 1995;**365**:371–6.
16. Naslain R. Concept of layered interphases in SiC_f/SiC. *Ceram Trans* 1995;**58**:23.
17. Bertrand S, Droillard C, Pailler R, Bourrat X, Naslain R. TEM structure of $(PyC/SiC)_n$ multilayered interphases in SiC_f/SiC composites. *J Eur Ceram Soc* 2000;**20**:1–13.
18. Kohyama A, Katoh Y. Effect of residual silicon phase on reaction-sintered silicon carbide. *Ceram Trans* 2002;**144**:3.
19. Naslain RR, Pailler R, Bourrat X, Bertrand S, Heurtevent F, Dupel P, Lamouroux F. Synthesis of highly tailored ceramic matrix composites by pressure-pulsed CVI. *Solid State Ionics* 2001;**141–142**:541–8.
20. Cofer CG, Economy J. Oxidative and hydrolytic stability of boron nitride – a new approach to improving the oxidation resistance of carbonaceous structures. *Carbon* 1995;**33**:389.
21. Arya SP, Damico A. Preparations, properties and applications of boron nitride thin films. *Thin Solid films* 1988;**157**:267–82.
22. Rebillat F, Le Gallet S, Guette A, Bourrat X, Naslain R. In: Krenkel W, et al., editors. *High temperature ceramic matrix composites*. Weinheim, Germany: Wiley-VCH; 2001. p. 193–8.
23. Matsuda T. Stability to moisture for chemically vapour-deposited boron nitride. *J Mater Sci* 1989;**24**:2353–8.
24. Gallet SL, Cholon G, Rebillat F, Guette A, Bourrat X, Naslain R, Couzi M, Bruncel JL. Micro structural and micro textural investigations of boron nitride deposited from BCl_3–NH_3–H_2 gas mixtures. *J Eur Ceram Soc* 2004;**24**:33.
25. Cholet V, Vandenbulcke L, Rouan JP, Baillif P, Erre R. Characterisation of boron nitride films deposited from BCl_3–NH_3–H_2 mixtures in chemical vapour infiltration conditions. *J Mater Sci* 1994;**29**:1417–35.
26. Rand MyronJ, Roberts JamesF. Preparation and properties of thin film boron nitride. *J Electrochem Soc, Solid State Sci* 1968;**115**(4):423–9.
27. Naslain R, Guette A, Rebillat F, Pailler R, Langlais F, Bourrat X. Boron-bearing species in ceramic matrix composites for long-term aerospace applications. *J Solid State Chem* 2004;**177**:449–56.
28. Naslain R. Fibre/matrix interphases and interfaces in ceramic matrix composites processed by CVI. *Compos Interfaces* 1993;**1**(3):253–86.
29. Naslain R. Interphases in ceramic matrix composites. *Ceram Trans* 1996;**79**:37–52.
30. Naslain R. The design of the fibre–matrix interfacial zone in ceramic matrix composites. *Composites A* 1998;**29A**:1145–55.
31. Naslain R, Dugne O, Guette A, Sevely J, Robin-Brosse C. Boron nitride interface in ceramic matrix composites. *Ceram Soc* 1991;**74**:2482.
32. Rocher J, Cotteret. Boron nitride interface in ceramic matrix composites. *J Am Ceram Soc* 1991;**74**:2482–8.
33. Lowden RA. Characterization and control of the fibre–matrix interface in ceramic matrix composites. ORNL-TM-11039. Sprinfield, VA: NTIS, US Dept. Commerce; March 1989.
34. Rebillat F, Guette A, Espitalier L, Debieuvre C, Naslain R. Oxidation resistance of SiC_f/SiC micro and mini composites with a highly crystallised BN interface. *J Eur Ceram Soc* 1998;**18**:1809–19.
35. Leparoux M, Vandelbulcke L, Clinard C. Influence of isothermal chemical vapour deposition and chemical vapour infiltration conditions on the deposition kinetics and structure of boron nitride. *J Am Chem Soc* 1999;**82**(5):1187–95.
36. Takeda M, Urano A, Sakamoto JC, Imai Y. Microstructure and oxidative degradation behavior of silicon carbide fibre Hi-Nicalon type S. *J Nucl Mater* 1998;**258–263**(2):1594–9.
37. Plucknett KP, Levis MH. Inhibition of intermediate temperature degradation of calcium aluminosilicate/Nicalon by high temperature pretreatment. *J Mater Sci Lett* 1995;**14**:1223–6.
38. Lin W, Yang J-M. Thermal stability of ceramic fibre in a CVI processed SiC matrix composite. *J Mater Sci* 1991;**26**:4116–22.
39. Xu Y, Cheng L, Zhang L, Yin H, Yin X. High toughness, 3D textile SiCf/SiC composites by CVI. *Mater Sci Eng* 2001;**A318**:183–8.
40. Leparoux M, Vandenbulcke L, Goujard S, Robin-Brosse C, Domergue JM. Mechanical behavior of 2D-SiC/BN/SiC processed by ICVI. In: *Proc. 10th Intern. Conference on Composite Materials, vol. IV*. 1995. p. 633–40.
41. *Ceramic fibres and coatings: advanced materials for the twenty-first century*. Washington, DC: National Academy Press; 1998. http://www.nap.edu/catalog/6042.html.
42. Leparoux M, Vandenbulcke L, Serin V, Sevely J, Goujard S, Robin-Brosse C. Oxidizing environment influence on the mechanical properties and microstructure of 2D—SiC/BN/SiC composites processed by ICVI. *J Eur Ceram Soc* 1998;**18**(6):715–23.